Field Induced Transitions in Rare Earth Intermetallic Compounds RX and RX_2 (R=Er, Ho, Dy, Tb and Gd and X=Ag and Au)(Magnetism)

Field Induced Transitions in Rare Earth Intermetallic Compounds RX and RX_2 (R = Er, Ho, Dy, Tb and Gd and X = Ag and Au)*

Takejirou Kaneko, Shunya Abe, Hajime Yoshida, Masayoshi Ohashi, Shigeto Miura, Giyuu Kido and Yasuaki Nakagawa

Institute for Materials Research, Tohoku University, Sendai
(Received February 12, 1993)

Synopsis

Rare earth intermetallic compounds RX and RX_2 (R = Gd, Tb, Dy, Ho and Er: X = Ag and Au) are antiferromagnetic compounds with the CsCl-type crystal structure and the $MoSi_2$-type one, respectively. Magnetization process is investigated for these compounds under static magnetic fields up to 270 kOe and pulsed ones up to 300 kOe. The observed field induced transitions are reviewed together with their magnetic phase diagrams.

I. Introduction

Rare earth metals (R) and noble metals (X) form a series of intermetallic compounds with formula RX, RX_2, RX_3 and RX_4. Extensive studies have been done by many authours[1], since the systematic investigation of the magnetic properties and their related properties of these compounds are useful for studying the indirect exchange interaction between magnetic ions embedded in crystals with a simple crystal structure together with ions of Ag or Au of relatively simple electronic configurations. The compounds RAg and RAu for heavy R have the crystal structure of a CsCl-type and are reported to be antiferromagnetic(AF) from the measurements of temperature dependence of magnetic susceptibility. Some of them have a magnetic order-order transition at the transition temperature(T_t) below the Neel temperature(T_N). The neutron diffraction studies show that TbAg has the commensurate (π π 0) AF structure below T_N[2], DyAg[3] and ErAg[4] the commensurate AF(1) structure below T_t and the sinusoidally modulated AF(2) one between T_t and T_N, and HoAg[5] the quasi-sinusoidally modulated AF(1) structure below T_t and the sinusoidally modulated AF(2) one between T_t and T_N. The temperature dependence of electrical resistivity was also studied for the above compounds[6,7] .

The values of T_t and T_N for RAg and RAu are obtained as following; T_t:T_N = -- : 155 K[8] for GdAg, -- : 106 K[9](100 K[2]) for TbAg, 46.6 K[10](46 K[3]) : 56.7 K[10](56 K[3]) for DyAg, (27 K[5]) : 33 K[10](33 K[5]) for HoAg, 9 K[10](9.5 K[4]) : 18.8 K[10](18 K[4]) for ErAg ; T_N = 23 K[10] for DyAu, 10 K[10] for HoAu and 16.5 K[10] for ErAu. T_N in the parentheses is from the results of neutron diffraction experiment.

For heavy rare earth elements the compounds RAg_2 and RAu_2 have the

---

* The 1920th report of Institute for Materials Research

tetragonal crystal structure of a $MoSi_2$-type, in which R atoms occupy the corner and body center positions. They are all known to be antiferromagnetic from the magnetic measurements. According to neutron diffraction studies by Atoji, $TbAg_2$[11] has the layer-type commensurate antiferromagnetic(AF) structure below T_N and $DyAg_2$[12], $TbAu_2$[13] and $DyAu_2$[12] the commensurate AF(1) structure below T_t and the incommensurate transverse wave AF(2) one between T_t and T_N.

The values of T_t and T_N are obtained to be T_t : T_N = -- : 34.4 K[14](-- : 35 K[11]) for $TbAg_2$, 9.5 K[14](9.5 K[12]) : 15 K(15 K) for $DyAg_2$, -- : 49.6 K[15,16] for $GdAu_2$, 43 K[15](42.5 K[13]) : 55 K(55 K) for $TbAu_2$ and 25 K[15](25.5 K[12]) : 31 K(33.8K) for $DyAu_2$.

In this report, we review our results of measurements of magnetization process for the intermetallic compounds RX and RX_2 (R = heavy rare earth elements and X = Ag and Au) under static magnetic fields up to 240 kOe and pulsed ones up to 300 kOe. The magnetic phase diagrams are also presented.

II. Experimental Procedures

All the specimens were prepared by arc-melting the mixtures of elements of formula proportion in an argon gas atmosphere and then annealed at 500 °C for 2-10 days.

Magnetization was measured using a vibrating-sample magnetometer under static magnetic fields up to 170 kOe which were generated by a water-cooled solenoid of the Bitter-type or using a sample extraction magnetometer under static magnetic fields up to 240 kOe which were generated by a hybrid magnet installed in High Field Laboratory for Superconducting Materials, IMR, Tohoku University. The magnetization was also measured under pulsed magnetic fields up to 300 kOe.

III. Experimental Results and Discussion

Figure 1 shows the magnetization curves of GdAg and TbAg measured under both static and pulsed magnetic fields[17]. Magnetizations of GdAg increase linearly with magnetic field as seen in the figure. No field induced transition was observed under the magnetic field employed in this experiment. The magnetization curve of TbAg at 95 K near T_N shows apparently an existence of field induced transition, which is considered to correspond to the transition from the AF state to the paramagnetic(P) one. The magnetization curve at 78 K shows a break from the linear part in low field region around 250 kOe, which indicates occurrence of the transition. The critical field H_c is defined here as the field of intersection of interpolations of the magnetization curves above and below the break. The temperature dependence of H_c of TbAg is shown in the inset of Fig. 1. H_c appears to decrease sharply just below T_N. Recently, Morin et al.[18] have reported that the transition of TbAg at T_N is of the first order transition from the results on temperature variations of magnetization, electrical resistivity and thermal conductivity. The sharp decrease of H_c near T_N is consistent with their results.

In Fig. 2 and 3 are shown the magnetization curves for DyAg under static magnetic field up to 150 kOe and pulsed one up to 300 kOe, respectively[17]. In the magnetization curve at 4.2 K under pulsed

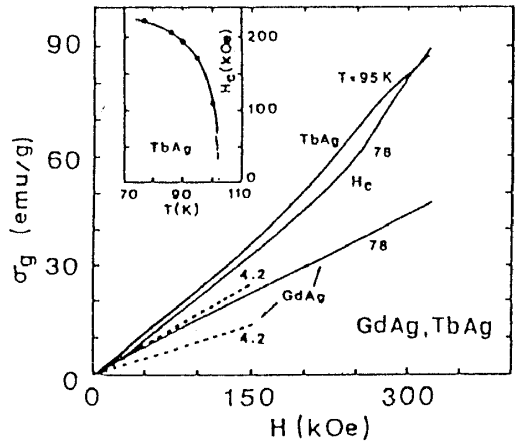

Fig. 1 Magnetization curves of GdAg and TbAg under static field up to 150 kOe and pulsed field up to 300 kOe. Inset: Magnetic phase diagram of TbAg.

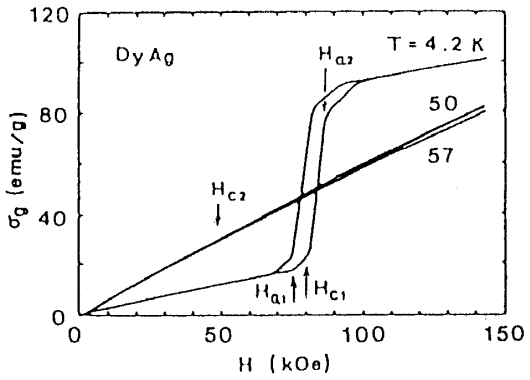

Fig. 2 Magnetization curves of DyAg under static magnetic field.

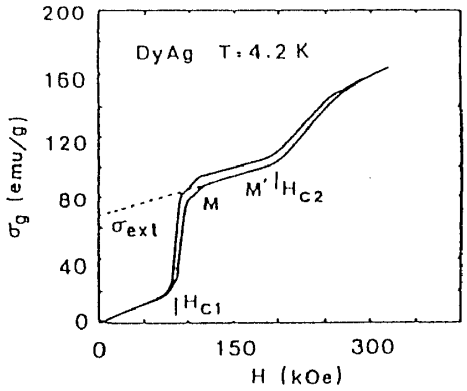

Fig. 3 Magnetization curves of DyAg under pulsed magnetic field.

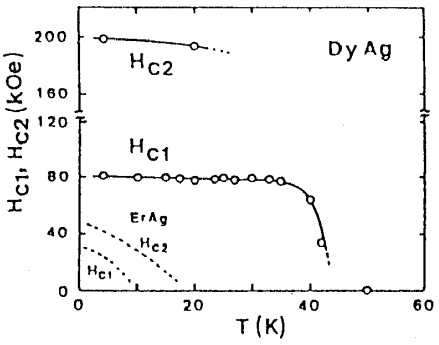

Fig. 4 Magnetic phase diagram of DyAg.

field there is observed apparently a two-stage field induced transition occurring at critical fields H_{c1} and H_{c2}. And then there are also observed anomalous magnetization processes around 75 kOe (H_{a1}) and 85 kOe (H_{a2}) in the magnetization curves under static field, which are considered to be due to field induced transition. The extrapolation of the part M-M' of the magnetization curve to zero field intersects the σ axis at a finite magnetization, σ_{ext}. This means that the transition is not that from the AF1 state with small susceptibility χ_{AF1} to the AF2 with large χ_{AF2} and the spin-flip transition corresponding to the change of the direction of AF spin axis, but there occurs the transition to an intermediate magnetic state with resultant ferromagnetic component induced by applying field. The value of σ_{ext} decreases with increase of temperature. The first transition and σ_{ext} disappear around T_t. The magnetization curve at 50 K between T_t and T_N shows only a one-stage field induced transition from the AF2 to the paramagnetic state. The transition is very gradual and then H_{c2} is not determined definitely at high temperatures. No field induced transition was observed at 57 K above T_N. The variations of H_{c1} and H_{c2}

with temperature are shown in Fig. 4, in which H_{c1} shows the sharp decrease around T_t. Recently, Morin et al.[19] have studied the magnetoelasticity and high field magnetization for the single crystal of DyAg. The measurements of magnetization were carried out in pulsed magnetic fields up to 400 kOe. They found that a two-stage field induced transition occurs along the [001] axis and a three-stage one along the [101] axis and [111] axes. They pointed out that the sequences under field of the different magnetic structures are mainly determined by the crystalline electric field and the antiferroquadrupolar interactions. The critical fields obtained for the polycrystalline sample in the present experiment, H_{a1}, H_{c1}, H_{a2} and H_{c2}, seem to correspond the H_{c1}[001], H_{c1}[111], H_{c1}[101] and H_{c2}[001] for the single crystalline sample, respectively. The transitions above 200 kOe were smeared out for the polycrystalline sample and were not detected.

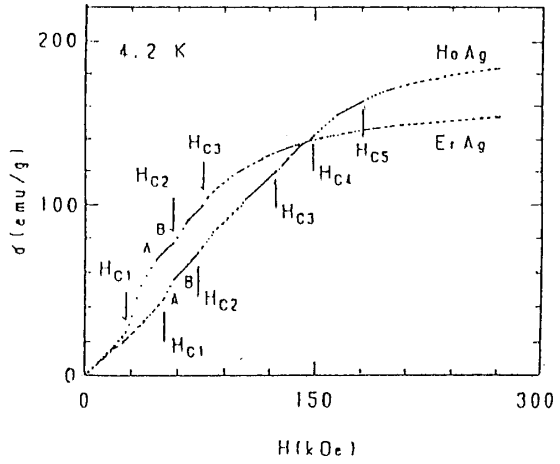

Fig. 5 Magnetization curves of HoAg and ErAg under static magnetic field at 4.2 K.

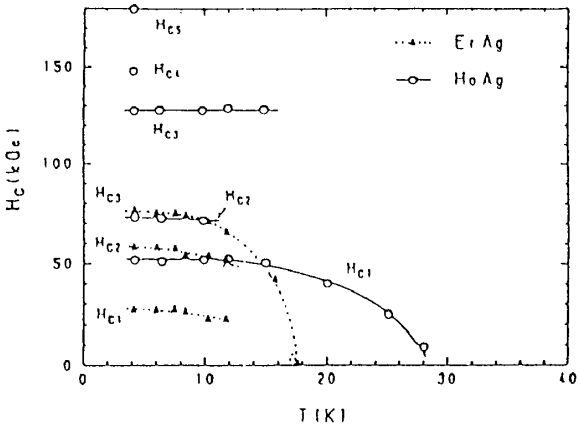

Fig. 6 Magnetic phase diagrams for HoAg and ErAg.

Figure 5 shows the magnetization curves of HoAg and ErAg at 4.2 K under static magnetic fields up to 270 kOe[20]. As seen in the figure, a multi-stage field induced transition occurs at the critical fields shown with arrows for both compounds. The transition fields at 4.2 K are obtained to be H_{c1} = 51 kOe and H_{c2} = 72 kOe, H_{c3} = 125 kOe, H_{c4} = 150 kOe and H_{c5} = 180 kOe for HoAg, and H_{c1} = 27 kOe, H_{c2} = 58 kOe and H_{c3} = 77 kOe for ErAg. Both magnetization curves appear to be saturated in fields above 200 kOe. The magnetic moment per Ho and Er ion estimated from the magnetization at 270 kOe is μ_{Ho} = 8.9 μ_B and μ_{Er} = 7.6 μ_B, respectively, which are comparable to those obtained in neutron diffraction measurements. The behavior of the first field induced transition for HoAg is somewhat different from that of DyAg and ErAg, since the extrapolation of the part A-B of the magnetization curve to zero field passes the origin. This field induced transition is considered to correspond to the transition from the AF1 state to the AF2 one as observed for $DyAu_2$ described later.[21] The magnetization process after the second field induced transition indicates that the different intermediate magnetic states appear after each transi-

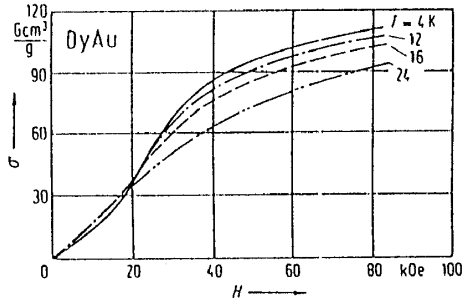

Fig. 7 Magnetization curves of DyAu under static magnetic field.

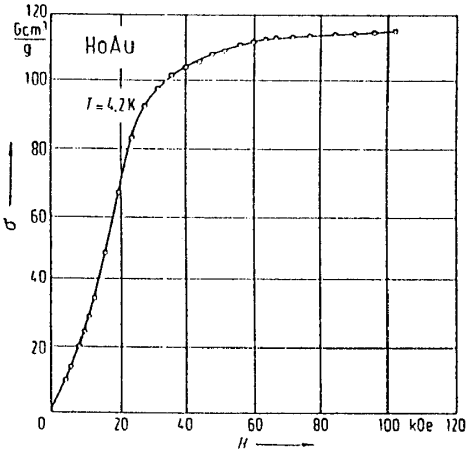

Fig. 8 Magnetization curve of HoAu under static magnetic field.

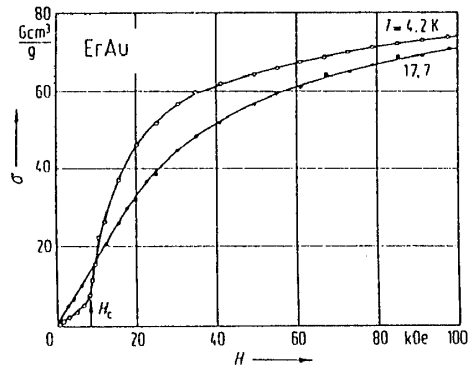

Fig. 9 Magnetization curves of ErAu under static magnetic field.

tion, since the extrapolation of the magnetization curve to zero field after each transition intersects the finite value of the σ axis. In the case of ErAg the extrapolation of the part A-B of the magnetization curve to zero field intersects the σ axis at a finite value for the magnetization. This behavior of the magnetization means that the first transition is one from the AF1 state to an intermediate magnetic state with a resultant ferromagnetic component like that observed for DyAg. The magnetization measurements at various temperatures were carried out under magnetic field up to 150 kOe. The temperature dependence of the critical fields thus obtained is shown in Fig. 6. The transition at H_{c2}, H_{c3}, H_{c4} and H_{c5} smeared out with increasing temperature, so that the temperature dependence of each critical field could not be determined at high temperatures.

Figures 7, 8 and 9 show the magnetization curves of DyAu, HoAu and ErAu, respectively[10]. There was observed only a one-stage field induced transition for these compounds contrast with the RAg compounds showing the multi-stage transition. The temperature dependence of H_c for ErAu is shown in Fig. 10 and those for DyAu and HoAu could not be determined definitely at high temperatures.

Figure 11 shows the magnetization curve for $GdAu_2$[10]. A field induced transition is observed around 50 kOe. The extrapolation of the high field part of the curve to zero field crosses the origin as seen in the figure. Then this transition corresponds to the spin-flip transition, where the AF spin axis changes to the direction perpendicular to the applied field from one parallel to the field. In Fig. 12 is shown the temperature dependence of H_c which corresponds to that of an anisotropy energy.

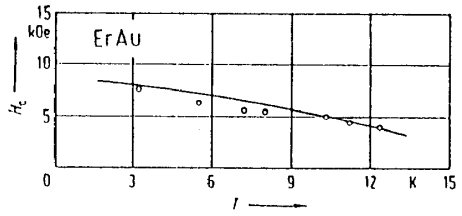

Fig. 10 Magnetic phase diagram of ErAu.

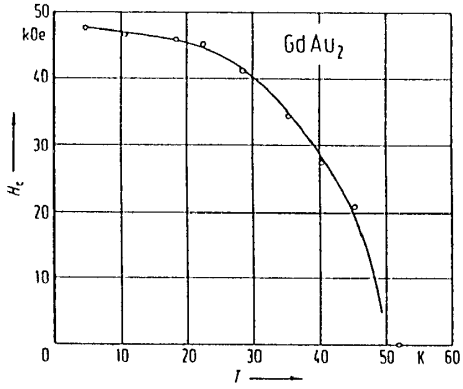

Fig. 12 Magnetic phase diagram of $GdAu_2$

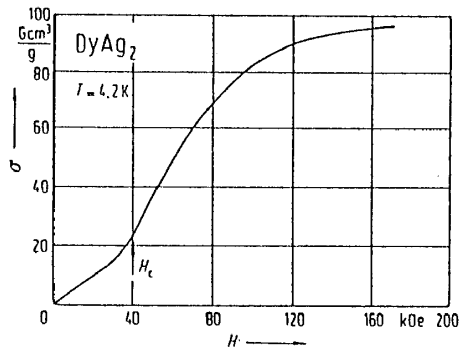

Fig. 14 Magnetization curve of $DyAg_2$ under pulsed magnetic field.

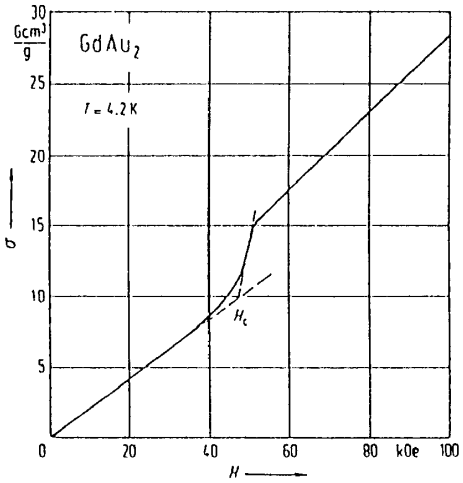

Fig. 11 Magnetization curve of $DyAu_2$ under static magnetic field.

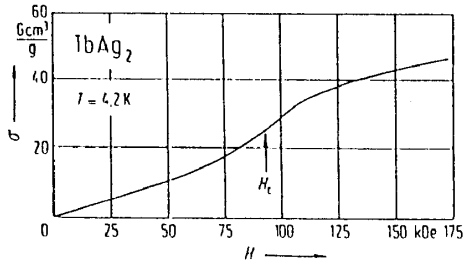

Fig. 13 Magnetization curve of $TbAg_2$ under pulsed magnetic field.

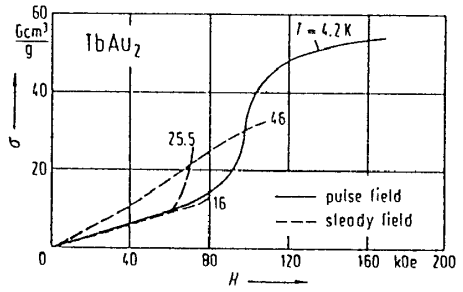

Fig. 15 Magnetization curves of $TbAu_2$ under static magnetic field and pulsed one.

Figures 13, 14, and 15 show the magnetization curves for $TbAg_2$, $DyAg_2$, $TbAu_2$[21]. There occur field induced transitions around 80 kOe ($TbAg_2$), 40 kOe ($DyAg_2$) and 100 kOe($TbAu_2$) , respectively. The observed field induced transitions appear like the transition from the AF state to the P one. On the other hand, the magnetization curve for $DyAu_2$ at 4.2 K in Fig. 16 shows a two-stage transition. The extrapolation of magnetization curve between 35 kOe to 50 kOe after the first transition crosses the origin and then this transition is considered to correspond to the transition from the AF1 state to the AF2 one. The field induced transitions above T_t are a one-stage transition from the AF2 state to the P one. From the magnetization curves in high field region the saturation magnetic moment μ_{sat} per R atom was estimated by using the law of approach to saturation. The obtained

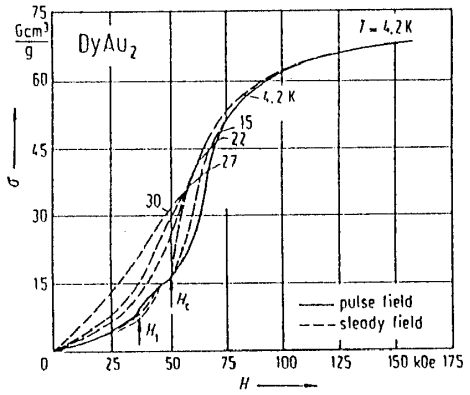

Fig. 16 Magnetization curves of $DyAu_2$ under static magnetic field and pulsed one.

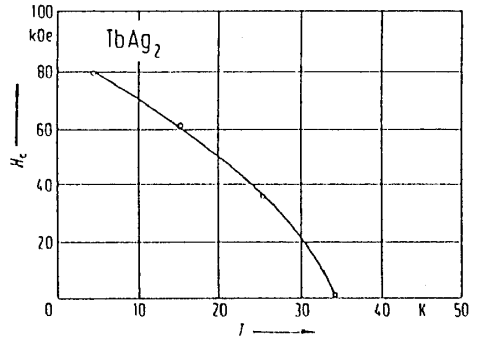

Fig. 17 Magnetic phase diagram of $TbAg_2$.

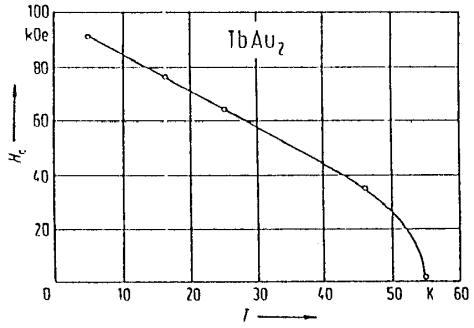

Fig. 18 Magnetic phase diagram of $TbAu_2$.

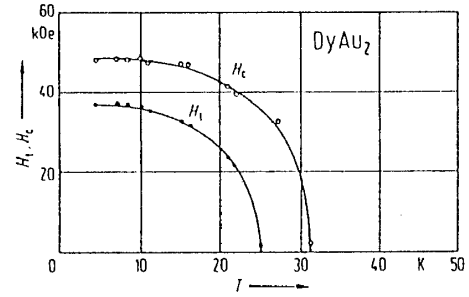

Fig. 19 Magnetic phase diagram of $DyAu_2$.

values are μ_{sat} = 4.3 μ_B (μ_{ND} = 8.95 μ_B from neutron diffraction experiment) for $TbAg_2$, 6.9 μ_B (7.44 μ_B) for $DyAg_2$, 6.0 μ_B (9 μ_B) for $TbAu_2$ and 7.2 μ_B (9.2 μ_B) for $DyAu_2$. All the estimated values of μ_{sat} are small compared with those of μ_{ND}. Especially the value of μ_{sat} in $TbAg_2$ is very small. This suggests that one more transition will occur for $TbAg_2$ with further increase of field. The magnetic phase diagrams are shown in Figs. 17, 18 and 19[20].

The multi-stage field induced transitions are observed for HoAg and ErAg as mentioned above. However, we can not discuss the mechanism of the transitions in details from the results for the polycrystalline samples as stated above about the transitions for DyAg. It is necessary to examine the magnetization process for the single crystalline sample to make clear the nature of the field induced transitions for the present compounds. The preparation of the single crystals are now in progress.

References

1) T. Kaneko, Landolt-Bornstein, III-vol.19e1, ed. H.P.J.Wijn, Springer-Verlag, Berlin, (1990) 1.
2) J.W.Cable, W.C.Koehler and E.O.Wollan, Phys.Rev., 136 (1964) A240.
3) T. Kaneko, H. Yoshida, M. Ohashi and S. Abe, J. Magn. Magn. Mater., 70 (1987) 277.

4) N. Nerson, J. Appl. Phys., 44 (1973) 4727.
5) P. Morin, D. Schmitt and C. Vettier, J. Phys.(Paris), 46 (1985) 39.
6) M. Ohashi, T. Kaneko, S. Miura and K. Kamigaki, J. Phys. Soc. Jpn., 34 (1973) 553.
7) C.C. Chao, J. Appl. Phys., 37 (1966) 2081.
8) H.B. Lal, J. Magn. Magn. Mater., 30 (1982) 192.
9) J. Pierre, R. Pauthenet, C. R. Acad. Sci., 260 (1965) 2739.
10) T. Kaneko, S. Abe, H. Yamauchi, H. Hiroyoshi and A. Hoshi, Proc. Int. Symp. on High Field Magnetism, ed. M. Date, North-Holland, Amsterdam, (1983) 105.
11) M. Atoji, J. Chem. Phys., 48 (1968) 3380.
12) M. Atoji, J. Chem. Phys., 51 (1969) 3877.
13) M. Atoji, J. Chem. Phys., 48 (1968) 560.
14) S. Miura, T. Kaneko, M. Ohashi and H. Yamauchi, J. Phys. Soc. Jpn., 37 (1974) 1464.
15) T. Kaneko, S. Miura, M. Ohashi and H. Yamauchi, Proc. Intern. Conf. Magnetism, 1973, Moscow, vol.5 Nauka, Moscow, (1974) 370.
16) T. Kaneko, S. Miura, M. Ohashi and K. Kamigaki, Proc. Int. Conf. Magnetism of Rare Earths and Actinides, ed. E. Burzo and M. Rogalski, Bucharest(1983) vol.1, (1983) 144.
17) S. Miura, T. Kaneko, S. Abe, G. Kido, H. Yoshida, K. Kamigaki and Y. Nakagawa, J. Phys.(Paris)Colloq., 49 (1988) C8-393.
18) P. Morin, J. Rouchy, M.M. Amado, R.P. Pinto, J.M. Moreira, V.S. Amaral, M.E. Braga and J.B. Sousa, J. Phys.(Paris)Colloq., 49 (1988) C8-395.
19) P. Morin, J. Rouchy, K. Yonenobu, A. Yamagishi and M. Date, J. Magn. Magn. Mater., 81 (1989) 147.
20) T. Kaneko, S. Abe, S. Sakurada, H. Yoshida, G. Kido and Y. Nakagawa, J. Magn. Magn. Mater., 104-107 (1992) 1401.
21) T. Kaneko, M. Ohashi, S. Miura, K. Kamigaki, A. Hoshi and H. Yoshida, AIP Conf. Proc., 24 (1975) 423.